MOEM

Modern Electronic Materials 2024; 10(1): 11–18
DOI 10.3897/j.moem.10.1.127026

Research Article

Study of cobalt ions diffusion in calcium orthovanadate crystal

Irina S. Voronina[1], Elizaveta E. Dunaeva[1], Liudmila I. Ivleva[1], Liudmila D. Iskhakova[1], Alexandr G. Papashvili[1], Maxim E. Doroshenko[1]

1 Prokhorov General Physics Institute of the Russian Academy of Sciences, 38 Vavilov Str., Moscow 119991, Russian Federation

Corresponding author: Irina S. Voronina (irina.voronina.78@list.ru)

Received 25 September 2023 ♦ **Accepted** 28 December 2023 ♦ **Published** 5 April 2024

Citation: Voronina IS, Dunaeva EE, Ivleva LI, Iskhakova LD, Papashvili AG, Doroshenko ME (2024) Study of cobalt ions diffusion in calcium orthovanadate crystal. *Modern Electronic Materials* 10(1): 11–18. https://doi.org/10.3897/j.moem.10.1.127026

Abstract

High-temperature diffusion doping has been used for the introduction of active cobalt ions in calcium orthovanadate $Ca_3(VO_4)_2$ single crystals (CVO). The test samples have been produced from nominally pure Cz CVO single crystals. High-temperature diffusion conditions have been optimized for the obtaining of doped optical quality single crystals in open or closed zone annealing. The diffusion coefficients of cobalt ions have been calculated for different conditions. Temperature regime, process time, diffusant type were defined. The samples have been annealed at 1150–1300 °C for 24–48 h with Co_3O_4, $Ca_{10}Co_{0.5}(VO_4)_7$ and $Ca_3(VO_4)_2$: 2 wt.% Co_3O_4 as diffusants. The diffusion direction has been parallel or perpendicular to the optical axis of the CVO crystal. The diffusion coefficients have been calculated to be in the range of $2.09 \cdot 10^{-8}$ – $1.58 \cdot 10^{-7}$ cm^2/s. The diffusion activation energies have been determined to be 2.58 ± 0.5 and 2.63 ± 0.5 eV for the [001] and [100] directions, respectively. The maximum cobalt concentration in the doped CVO crystals has been found to be $2 \cdot 10^{20}$ cm^{-3}. The absorption spectrum of the diffusion doped $Ca_3(VO_4)_2$: Co samples has exhibited absorption bands typical of the Co^{2+} and Co^{3+} ions. It has been shown that the intensity ratio between the characteristic absorption bands varies depending on crystal obtaining technique. The optical anisotropy of the crystal increases with dopant concentration.

Keywords

diffusion, doping, cobalt ions, high-temperature annealing, calcium orthovanadate, optical properties

1. Introduction

The fabrication of active elements for solid state lasers and laser systems having good performance in a wide spectral range is based on the synthesis of doped high optical quality single crystals. Calcium orthovanadate $Ca_3(VO_4)_2$ single crystals possess a number of properties finding applications in laser engineering:

– possibility of introducing laser activator ions in concentrations providing the efficient laser radiation generation [1–5];

– high efficiency nonlinear laser radiation conversion, high radiation resistance and Raman gain [6];

– high-temperature ferroelectric crystal with a specific domain structure [7].

Earlier [8, 9] the concentration series of $Ca_3(VO_4)_2$: Mn and $Ca_3(VO_4)_2$: Co crystals were grown and it was shown that the growth of crystals with high transition metal concentrations is a complex task requiring the bulk growth rate be significantly reduced.

Multiple methods of dopant introduction into as-grown crystals have been developed, e.g. radiation doping, ion

implantation, gaseous, liquid or solid state diffusion methods. The obtained semiconductor crystals has been studied most thoroughly, and they are widely used, e.g. for the fabrication of solar cells [10, 11]. A^2B^6 matrices diffusion doped with transition metals (Cr^{2+}, Fe^{2+}) are well-known as materials for laser engineering [12–15]. However, diffusion processes in oxide crystals has not been studied sufficiently yet. Diffusion of active ions in lithium niobate, yttrium vanadate and garnets was studied [16–19]. The typical diffusion rates in those crystals are quite low, resulting in small impurity penetration depths. The fabrication of large-size doped crystals is a time-consuming task. It should be noted that ion implantation and radiation doping processes often deteriorate the crystal structure of doped regions and generate thermal defects. The formation of crystal regions with the desired doping impurity distribution and arrangement is typically achieved via additional heat treatment (annealing) [8]. The high-temperature diffusion method can be used for the introduction of doping impurities into nominally pure crystals. The impurity sources can be compounds in solid, liquid or gaseous states (diffusants). Diffusion can occur from a permanent external source or from a finite surface source. Diffusion obeys Fick's laws [20]. Impurities are characterized by diffusion coefficients D. The higher the diffusion coefficient D, the faster is diffusion and the shorter time is required for synthesizing an activated layer with the desired thickness. Longer diffusion produces a concentration plateau corresponding to the impurity solubility limit. However, in most cases the actual impurity distribution has a complex profile since the diffusion coefficient depends on vacancy/impurity concentrations and on deviation of the diffusion coefficient temperature dependence from Arrhenius' law. The key requirement to actively doped oxide materials is a highly homogeneous dopant distribution in the crystal. Studies of the actual structure of diffusion-doped crystals and the processes occurring therein require taking into account the diffusion coefficients of intrinsic ions and impurity atoms. Calcium orthovanadate $Ca_3(VO_4)_2$ (CVO) crystals are of interest for studying diffusion processes. CVO crystals have a whitlockite structure, crystallizing in the non-centrosymmetric space group $R3c$ [21, 22]. Their structure contains six different Ca^{2+} cation sites four of which are occupied, one is vacant and one is half-occupied. Thus, the presence of a large number of cation vacancies provides the possibility of isovalent and heterovalent substitutions without changing the space group $R3c$ which is important for the formation of the desired properties. CVO is known to have a high ionic conductivity which increases even further in the presence of trivalent ions in the structure [23].

Cobalt is of interest as an activator ion since it can have different oxidation degrees ($Co^{2+}/Co^{3+}/Co^{4+}$) and occupy tetrahedral and octahedral sites in CVO due to its small ionic radius [9] thus providing the possibility of modifying the luminescent properties of the material. Co^{2+} doped CVO crystals can provide for passive Q-factor modulation due to nonlinear transmittance [24]. The aim of this work is to study the possibility of CVO : Co fabrication using high-temperature diffusion annealing in cobalt oxide and calcium/cobalt vanadates having different chemical compositions.

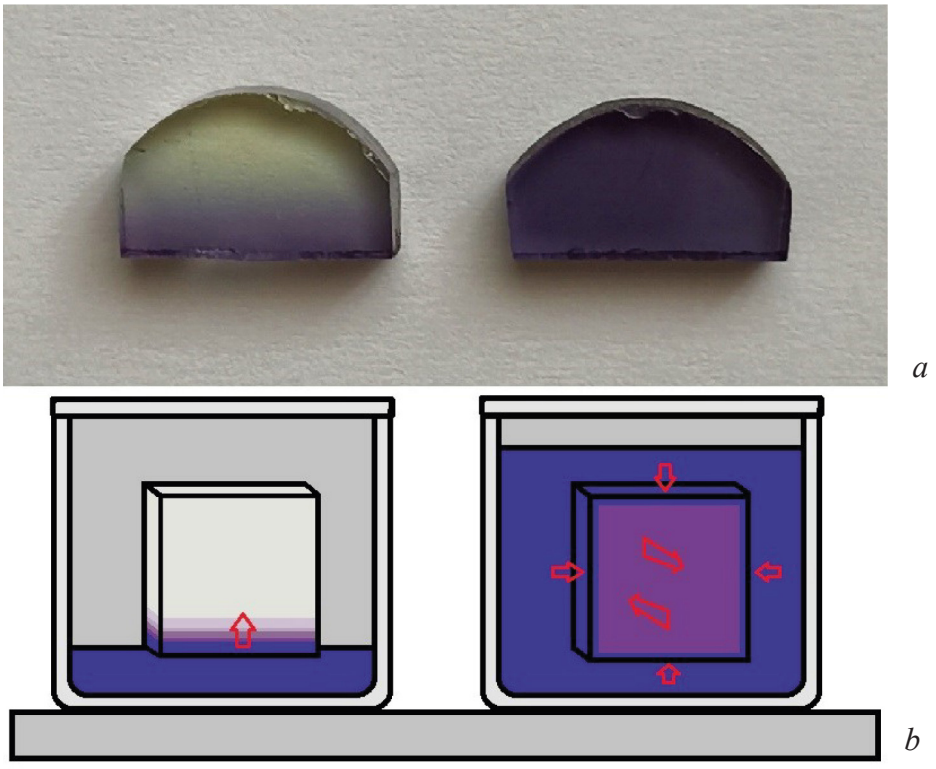

Figure 1. (*a*) Appearance of CVO crystals and (*b*) diffusion doping schematic in (left) open zone and (right) closed zone

2. Experimental

Solid-state high-temperature diffusion method was used for dopant introduction into CVO single crystals. The test samples were made from Cz-grown high optical quality nominally pure CVO crystals. The ~12 × 10 × 2 mm^3 sized CVO crystal samples were placed in a ceramic container filled with diffusant, i.e., a cobalt ion containing compound. High-temperature diffusion doping of the CVO crystals was carried out using two diffusion techniques (Fig. 1):

– in an open zone (the crystal is placed on powdered diffusant and exposed to air);

– in a closed zone (the crystal is completely covered with diffusant powder and does not contact with air).

The annealing temperature was varied between 1150 and 1300 °C, and the annealing time, from 24 to 48 h. Diffusion occurred parallel and perpendicular to the *C* axis. For open zone annealing, a diffusing ion concentration profile forms, allowing one to calculate the diffusion coefficient. Closed zone annealing provides for the maximum doping ion concentration in the crystal and eliminates volatile component loss (in the case considered, vanadium). After annealing the sample was slowly cooled in order to avoid the generation of thermal stresses and cracking.

The diffusants were selected using the following criteria:

– sufficient cobalt content;

– melting point is higher than effective diffusion annealing temperature (approx. 1200–1300 °C for $Ca_3(VO_4)_2$);

– no introduction of extrinsic ions;

– no chemical transformations at working temperatures, until the annealing temperature.

Of all the calcium, cobalt and vanadium compounds, only $Ca_3(VO_4)_2$: 2 wt.% Co_3O_4 meets the above criteria, and it was used in our earlier single crystal growth experiments [9]. Diffusion annealing was also carried out in Co_3O_4 and $Ca_{10}Co_{0.5}(VO_4)_7$ media, but those compounds interact with the sample surface during annealing. Cobalt oxide Co_3O_4 undergoes chemical decomposition with oxygen release at above ~950 °C:

$$2Co_3O_4 \rightarrow 6CoO + O_2\uparrow,$$

and the $Ca_{10}Co_{0.5}(VO_4)_7$ compound which is close to $Ca_3(VO_4)_2$ by composition has a whitlockite structure [25] but undergoes intense oxidation at 1300 °C. In either case the sample surface is strongly damaged. However, the use of the above diffusants provides for higher doping ion concentrations in the test samples. Compounds having lower melting points [26, 27] were not used.

The concentration profiles of the main elements and the transition metal along the crystal were monitored using energy dispersion X-ray spectroscopy (EDXS) with an AZtecENERGY Analytical Systems attachment (Oxford Instruments) on a JSM5910-LV scanning electron microscope (JEOL) at a 20 kV acceleration voltage. The polished samples were coated with an electrically conducting carbon layer before the tests. The reference was a $Ca_3(VO_4)_2$ single crystal with an X-ray proven phase purity, the verified unit cell parameters being close to those reported earlier [8]. The Ca, V and Co concentration determination errors were 0.05, 0.06 and 0.03 at.%, respectively.

The absorption spectra were studied at room temperature on a CARY-5000 spectrophotometer.

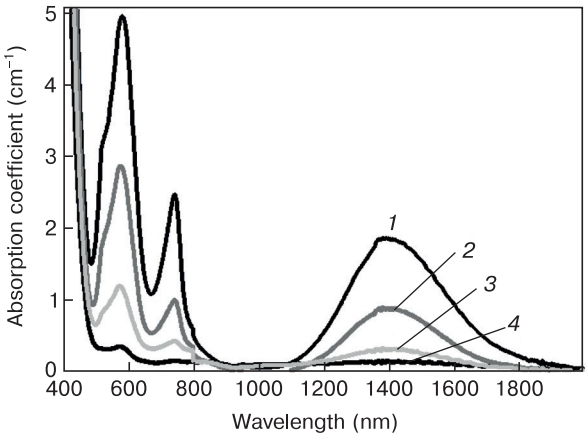

Figure 2. Cobalt ion absorption spectra for CVO samples as a function of diffusion distance, taken with 1.5 mm diam. Diaphragms: (*1*) *x* = 2 mm, (*2*) 3.5, (*3*) 5 and (*4*) 6.5

3. Results and discussion

3.1. Diffusion coefficient calculation

Earlier studies of manganese diffusion in CVO [28] showed that annealing at below 1050 °C does not ensure efficient impurity penetration in the crystal bulk since the diffusion coefficients are very low. Diffusion at above 1300 °C causes thermal etching of the wafer surfaces thus significantly reducing their quality. Furthermore, high-temperature annealing generates point defects (vacancies and interstitial atoms). Therefore the optimum diffusion annealing temperature range for CVO crystals was chosen at 1150–1300 °C.

The room temperature cobalt ion depth profiles in the CVO crystals can well be seen from the experimental absorption spectra. The measurement points were exactly selected using special 1.5 mm diam. diaphragms. Figure 2 shows the absorption spectra of cobalt ions in the CVO samples.

The cobalt ion diffusion profile in CVO after open-zone diffusion annealing is described by the second Fick law which depends on annealing conditions. Our experimental conditions are best described by a monodimensional model of diffusion from a thin layer to a semi-closed

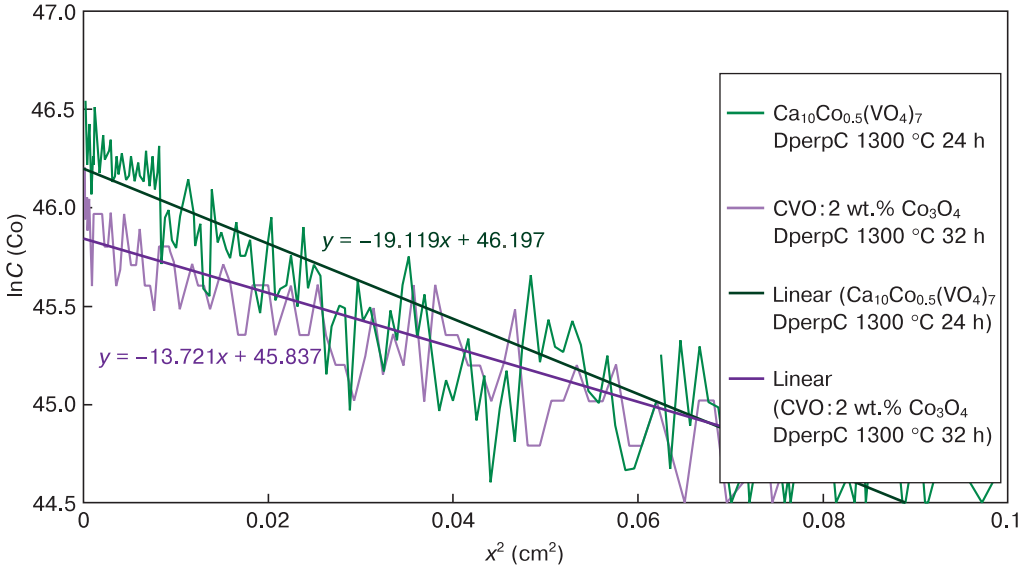

Figure 3. $\ln C(\mathrm{Co}) = f(x^2)$ dependences

space. The diffusion equation for those conditions is as follows [20, 29]:

$$C(x,t) = \frac{M}{\sqrt{\pi Dt}} \exp\left[\frac{x^2}{4Dt}\right], \quad (1)$$

where $C(x, t)$ is the impurity concentration at the depth x and the time t; M is the number of particles per unit area; D is the diffusion coefficient.

The following expressions can be obtained from Eq. (1) for similar time t and different penetration depths x_1 and x_2:

$$\ln C(x_1) = \ln \frac{M}{\sqrt{\pi Dt}} \frac{x_1^2}{4Dt},$$

$$\ln C(x_2) = \ln \frac{M}{\sqrt{\pi Dt}} \frac{x_2^2}{4Dt}. \quad (2)$$

Thus,

$$\ln C(x_1) - \ln C(x_2) = \frac{-\left(x_1^2 - x_2^2\right)}{4Dt};$$

$$D = \frac{-\frac{1}{4t}\left(x_1^2 - x_2^2\right)}{\ln C(x_1) - \ln C(x_2)}. \quad (3)$$

The parameter $(\ln C(x_1) - \ln C(x_2))/(x_1^2 - x_2^2) = \mathrm{tg}(\delta)$ can be determined from the dependence $\ln(C) = f(x^2)$, where x is the distance from the diffusion source and C is the cobalt ion concentration per 1 cm^3 of crystal bulk. Figure 3 shows examples of the obtained dependences.

Cobalt diffusion coefficients in CVO were determined from Eq. (3) and the calculated $\ln C(\mathrm{Co}) = f(x^2)$ tangents.

3.2. Chemical composition of doped crystals

The chemical compositions of the as-diffusion annealed crystals were determined using energy dispersion X-ray spectroscopy (EDXS). The depth profiles of the main elements and cobalt are shown in Fig. 4.

It can be seen from Fig. 4 that the cobalt concentration decreases in depth from 0.25±0,02 at.% to zero. The calcium concentration increases from 22.85±0.06 to 23.02±0.06 at.%, i.e., by 0.27±0.06 at.%, whereas the

Table 1. Cobalt diffusion coefficients calculated for different CVO sample annealing conditions

Diffusion direction	Annealing temperature (°C)	Annealing time (h)	Diffusion coefficient (cm²/s)
$D \perp C$, layer $Ca_3(VO_4)_2$: 2 wt.% Co_3O_4	1150	48	$(2.09 \pm 0.3) \cdot 10^{-8}$
	1200	48	$(4.21 \pm 0.6) \cdot 10^{-8}$
	1300	32	$(1.58 \pm 0.1) \cdot 10^{-7}$
$D \perp C$, layer $Ca_{10}Co_{0.5}(VO_4)_7$	1300	24	$(1.51 \pm 0.1) \cdot 10^{-7}$
$D \parallel C$, layer $Ca_3(VO_4)_2$: 2 wt.% Co_3O_4	1150	48	$(2.37 \pm 0.3) \cdot 10^{-8}$
	1200	48	$(4.66 \pm 0.6) \cdot 10^{-8}$
	1250	48	$(9.74 \pm 1.2) \cdot 10^{-8}$

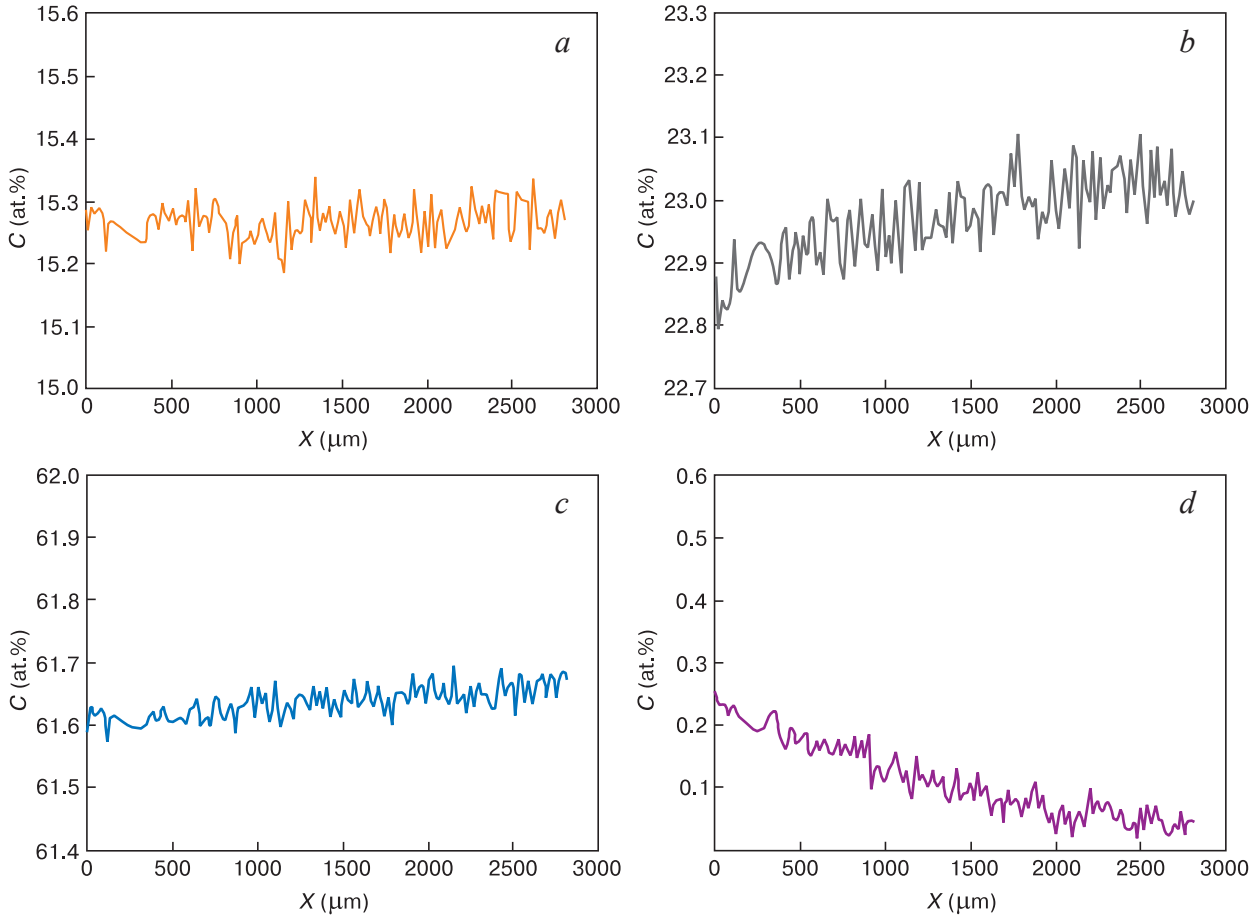

Figure 4. Depth profiles of main elements (*a*) V, (*b*) Ca, (*c*) O and (*d*) Co for $Ca_3(VO_4)_2$:Co sample annealed in open space with $Ca_{10}Co_{0.5}(VO_4)_7$ powder at 1300 °C for 24 h

vanadium concentration remains constant. The cobalt concentration changes to the same extent as the calcium concentration, i.e., cobalt ions substitute calcium ones but do not substitute vanadium ones. The slight oxygen depletion can be caused by vacancies generated in the presence of Co^{3+} ions in the crystal. It was shown earlier for $Ca_3(VO_4)_2$:Mn crystals synthesized using diffusion annealing under similar conditions [28] that manganese diffusion into the CVO crystal changed both the calcium and vanadium concentrations. Thus, unlike cobalt, manganese enters both the cation and the anion sublattices. The different behavior patterns of those transition metal ions can be accounted for by manganese ability to take on an oxidation degree of 5+ thus facilitating its incorporation into VO_4^{2-} anions.

According to EDXS data, the maximum cobalt content in the CVO crystals, i.e., 0.29 at.% ($2 \cdot 10^{20}$ cm^{-3}), was achieved via closed zone annealing of Co_3O_4 at T = 1300 °C for 24 h. Doping of $Ca_3(VO_4)_2$: 2 wt.% Co_3O_4 provided for a highest Co concentration of 0.15 at.% in the crystals. The maximum cobalt concentration in the crystal Cz-grown from $Ca_3(VO_4)_2$: 2 wt.% Co_3O_4 melt was 0.1 at.%.

3.3. Diffusion activation energy

Diffusion coefficient has the following diffusion temperature dependence [20]:

$$D = D_0 \exp\left(\frac{E_a}{kT}\right), \quad (4)$$

where E_a is the activation energy; $k = 8.617 \cdot 10^{-5}$ eV/K [12] is Boltzmann's constant; T is the temperature, K; $D_0 = \mu\beta^2\exp[S/(kT)]$ is the pre-exponential factor; S is the activation entropy; m is the structure-dependent geometrical factor; $\beta \sim 3 \cdot 10^{-8}$ cm is the unit jump length [20]. Equation (4) allows one to evaluate the activation energy and the pre-exponential factor.

It follows from Eq. (4) that

$$\ln D = \ln D_0 - \frac{E_a}{kT}; \quad (5)$$

$$E_a = -k\frac{\ln D(T_1) - \ln D(T_2)}{\frac{1}{T_1} - \frac{1}{T_2}}. \quad (6)$$

The parameter $[\ln D(T_1) - \ln D(T_2)]/(1/T_1 - 1/T_2) = \mathrm{tg}(\delta)$ can be determined from the dependence $\ln D = f(1/T)$ (Fig. 5).

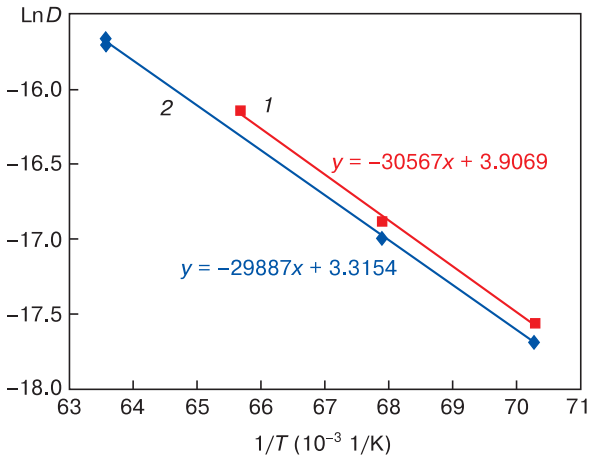

Figure 5. ln$D$ = $f(1/T)$ dependences for CVO crystals after open-zone diffusion annealing at 1150, 1200, 1250 и 1300 °C for (*1*) $D\|C$ and (*2*) $D\perp C$

The diffusion activation energy as determined from Fig. 5 and Eq. (6) depends but slightly on the diffusion direction (parallel or perpendicular to the optical axis) and is 2.58 ± 0.5 and 2.63 ± 0.5 eV for $D\perp C$ and $D\|C$, respectively. The diffusion activation energy E_a of semiconductor crystals is known to be about 3–4 eV for vacancy mechanism and about 0.6–1.2 eV for interstitial mechanism [29]. As a rule, the smaller the effective ionic radius of the doping ions, the more readily it diffuses in the crystal lattice and hence the lower E_a. Thus, the calculated activation energies for the case considered suggest that the cobalt diffusion mechanism in the test crystals is combined. The diffusion activation

Table 2. Ionic radii of manganese and cobalt as compared with those of calcium and vanadium [30]

Ion	Ionic radium (nm)	Ion	Ionic radium (nm)
Octahedral site		*Tetrahedral site*	
Ca^{2+}	0.1	V^{5+}	0.036
Mn^{2+}	0.067	Mn^{5+}	0.033
Mn^{3+}	0.058		
Co^{2+}	0.065	Co^{4+}	0.040 (not found in crystal)
Co^{3+}	0.055		

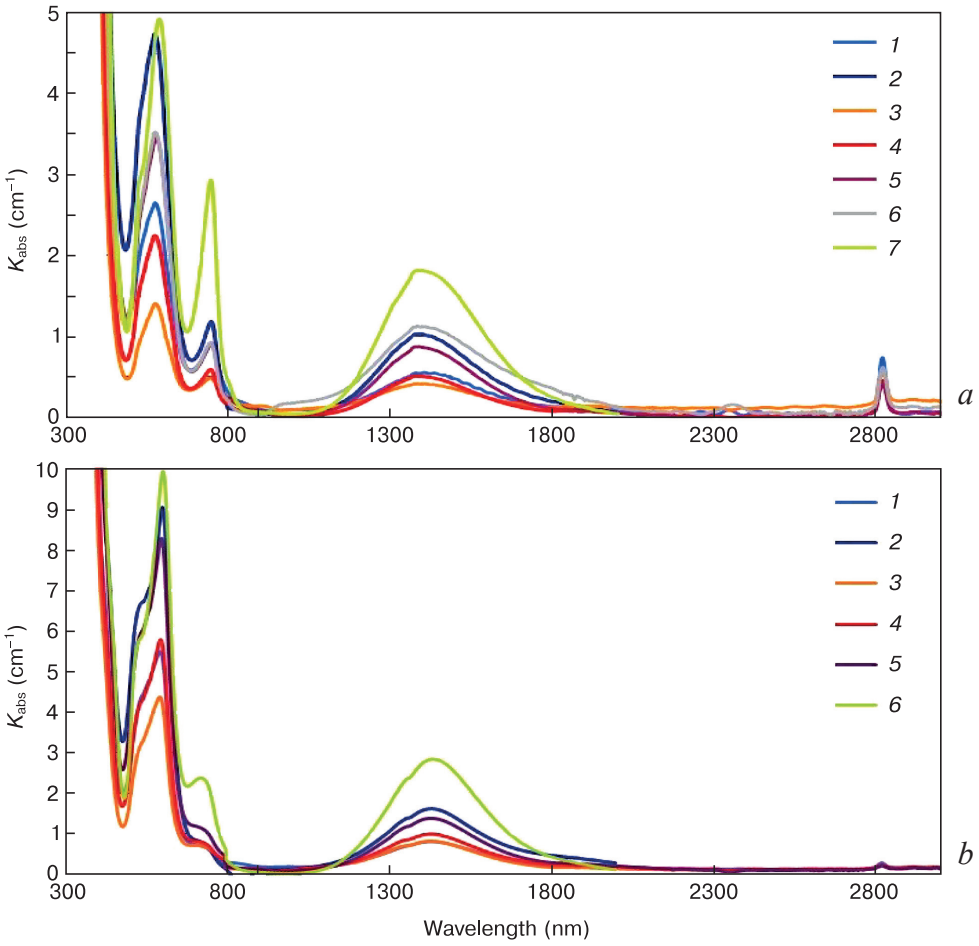

Figure 6. Absorption spectra of doped $Ca_3(VO_4)_2$: Co crystals for (*a*) $E\|C$ and (*b*) $E\perp C$ orientations: *a*: (*1*, *2*) $Ca_3(VO_4)_2$: 1 and 2% Co_3O_4, respectively, Cz-grown; (*3–5*) $Ca_3(VO_4)_2$: 2 % Co_3O_4, open zone diffusion annealing at (*3*) 1150, (*4*) 1200 and (*5*) 1250 °C for 24 h; (*6*) $Ca_3(VO_4)_2$: 2 % Co_3O_4, open zone diffusion annealing at 1300 °C for 32 h; (*7*) diffusion from Co_3O_4, 24 h, 1300 °C; *b*: (*1*, *2*) $Ca_3(VO_4)_2$: 1 and 2 % Co_3O_4, respectively, Cz-grown; (*3–5*) $Ca_3(VO_4)_2$: 2% Co_3O_4, open zone diffusion annealing at (*3*) 1150, (*4*) 1200 and (*5*) 1250 °C for 24 h; (*6*) diffusion from Co_3O_4, 24 h, 1300 °C

energies for $Ca_3(VO_4)_2$: Mn in our earlier experiments [28] differed significantly depending on sample orientation (3.3 ± 0.4 eV and 1.7 ± 0.4 eV for the $D \perp C$ and $D \| C$ directions, respectively). Since the ionic radii of manganese and cobalt are quite close (Table 2), the new data on cobalt diffusion require additional studies.

One can assume that small-sized Mn^{5+} ions contribute to manganese diffusion since they can readily diffuse over interstitial sites.

3.4. Spectroscopic studies

The absorption spectra of the $Ca_3(VO_4)_2$: Co crystals fabricated by diffusion annealing in open zone were compared with those of CVO doped by cobalt during Cz growth (Fig. 6).

One can separate characteristic absorption bands in the absorption spectra at 570 and 740 nm and in the 1200–1800 nm range. Studies of Cz-grown $Ca_3(VO_4)_2$: Co crystals showed that post-growth annealing at 850 °C increases the absorption band at 570 nm, while vacuum annealing, on the contrary, increases the absorption bands at 740 and 1200–1800 nm [9]. One can assume that the 570 nm absorption band is caused by Co^{3+} ions whereas the 740 and 1200–1800 nm ones, by Co^{2+} ones. It can be seen from the spectra shown in Fig. 6 that the 570/740 nm and 570/1200–1800 nm absorption band intensity ratios differ between the crystals after diffusion annealing in Co_3O_4, $Ca_3(VO_4)_2$: 2 wt.% Co_3O_4 and the Cz-grown ones. After annealing in Co_3O_4 the absorption bands typical of Co^{2+} are the strongest. One can assume that the crystal is under slightly reducing conditions for closed-zone annealing. After Cz growth, the strongest absorption band is the 570 nm one which is typical of Co^{3+}. The test crystals also have a 2825 nm absorption peak typical of OH^- groups.

Earlier studies of fluorescence spectra for $Ca_3(VO_4)_2$: Co crystals [9] showed that 532 nm excitation produces a 1170 nm fluorescence peak for Cz-grown and diffusion annealed crystals. The broad IR fluorescence peak is attributed to Co^{2+} ions. The fluorescence extinction kinetics can be represented as a sum of two components with lifetimes of 13 ms (corresponding to Co^{2+}) and 3 ms (attributable to Co^{3+}). It was concluded from the results that the crystal has two types of octahedral optical centers with different octahedral distortions.

4. Conclusion

High-temperature diffusion doping was for the first time used for fabrication of cobalt ion doped calcium orthovanadate crystals. The cobalt diffusion coefficients were determined for different temperatures, and the diffusion activation energies were calculated. Cobalt diffusion rate is shown to depend but slightly on diffusion direction in the test material. It was assumed that cobalt diffusion in CVO crystals occurs by both interstitial and vacancy mechanisms.

The absorption and fluorescence spectra of the doped crystals suggest the presence of both Co^{2+} and Co^{3+} ions. High-temperature diffusion annealing in Co_3O_4 increases the 700 and 1500 nm absorption peaks which are typical of Co^{2+} and provides for the maximum cobalt concentration in the crystals ($2 \cdot 10^{20}$ cm^{-3}). $Ca_3(VO_4)_2$: 2 wt.% Co_3O_4 proved to be a solid state diffusant protecting the sample surface during annealing. The cobalt concentration in the doped crystal is 1.5 times higher that in the crystal Cz-grown from same-composition melt.

Acknowledgements

This work was supported by the Russian Science Foundation (Project No. 23-23-00383, https://rscf.ru/project/23-23-00383/).

References

1. Brixner L.H., Flournoy P.A. Calcium orthovanadate $Ca_3(VO_4)_2$ – A new laser host crystal. *Journal of the Electrochemical Society.* 1965; 112(3): 303–308. https://doi.org/10.1149/1.2423528
2. Wu H.-F., Yuan F., Sun Sh., Huang Y., Zhang L., Lin Zh., Wang G. Growth and spectral characteristics of a new promising stoichiometric laser crystal: $Ca_9Yb(VO_4)_7$. *Journal of Rare Earths*. 2015; 33(3): 239–243. https://doi.org/10.1016/S1002-0721(14)60409-9
3. Kosmyna M.B., Nazarenko B.P., Puzikov V.M., Shekhovtsov A.N., Paszkowicz W., Behrooz A., Romanowski P., Yasukevich A.S., Kuleshov N.V., Demesh M.P., Wierzchowski W., Wieteska K., Paulmann C. $Ca_{10}Li(VO_4)_7$:Nd^{3+}, a promising laser material: growth, structure and spectral characteristics of a Czochralski-grown single crystal. *Journal of Crystal Growth*. 2016; 445: 101–107. https://doi.org/10.1016/j.jcrysgro.2016.04.002
4. Ivleva L.I., Dunaeva E.E., Voronina I.S., Doroshenko M.E., Papashvili A.G. $Ca_3(VO_4)_2$:Tm^{3+} – A new crystalline medium for 2-μm lasers. *Journal of Crystal Growth*. 2018; 501: 18–21. https://doi.org/10.1016/j.jcrysgro.2018.08.019
5. Ivleva L.I., Dunaeva., E.E., Voronina I.S., Doroshenko M.E., Papashvili A.G., Sulc J., Kratochvíl J., Jelinkova H. Impact of Tm^{3+}/Ho^{3+} co-doping on spectroscopic and laser properties of $Ca_3(VO_4)_2$ single crystal. *Journal of Crystal Growth*. 2019; 513: 10–14. https://doi.org/10.1016/j.jcrysgro.2019.02.054
6. Frank M., Smetanin S.N., Jelínek Jr.M., Vyhlídal D., Ivleva L.I., Dunaeva E.E., Voronina I.S., Shukshin V.E., Zverev P.G., Kubeček V. Synchronously-pumped, all-solid-state, picosecond Raman laser at 1169 and 1222 nm on single and combined Raman modes in a $Ca_3(VO_4)_2$ crystal with 30-times pulse shortening down

to 1.2 ps. *Laser Physics Letters*. 2020; 17(11): 115402. https://doi.org/10.1088/1612-202X/abbedf

7. Glass A.M., Abrahams S.C., Ballman A.A., Loiacono G. Calcium orthovanadate, $Ca_3(VO_4)_2$ - A new high temperature ferroelectric. *Ferroelectrics*. 1977; 17(1): 579–582. https://doi.org/10.1080/00150197808236782
8. Voronina I.S., Voronov V.V., Dunaeva E.E., Iskhakova L.D., Papashvili A.G., Doroshenko M.E., Ivleva L.I. Growth and properties of manganese doped $Ca_3(VO_4)_2$ single crystals. *Journal of Crystal Growth*. 2021; 555: 125965. https://doi.org/10.1016/j.jcrysgro.2020.125965
9. Voronina I.S., Dunaeva E.E., Papashvili A.G., Doroshenko M.E., Ivleva L.I. Modification of calcium orthovanadate single crystal due to cobalt doping. *Journal of Crystal Growth*. 2023; 615(3): 127242. https://doi.org/10.1016/j.jcrysgro.2023.127242
10. Bracht H. Diffusion mechanisms and intrinsic point-defect properties in silicon. *MRS Bulletin*. 2000; 25(6): 22−27. https://doi.org/10.1557/mrs2000.94
11. Kozlov V.A., Kozlovski V.V. Doping of semiconductors using radiation defects produced by irradiation with protons and alpha particles. *Semiconductors*. 2001; 35: 735–761. https://doi.org/10.1134/1.1385708
12. Mirov S.B., Fedorov V.V., Martyshkin D.V., Moskalev I.S., Mirov M.S., Gapontsev V.P. Progress in mid-IR Cr^{2+} and Fe^{2+} doped II-VI materials and lasers [Invited]. *Optical Materials Express*. 2011; 1(5): 898–910. https://doi.org/10.1364/OME.1.000898
13. Vaksman Yu.F., Pavlov V.V., Nitsuk Yu.A., Purtov Yu.N., Nasibov A.S., Shapkin P.V. Optical absorption and chromium diffusion in ZnSe single crystals. *Semiconductors*. 2005; 39(4): 377–380. https://doi.org/10.1134/1.1900247
14. Rodin S.A. Diffusion doping of CVD-ZnSe with Cr^{2+} ions. Diss. Cand. Sci. (Chem.). Nizhnii Novgorod; 2018. 129 p. (In Russ.)
15. Sorokina T. Cr^{2+}-doped II-VI materials for lasers and nonlinear optics. *Optical Materials*. 2004; 26(4): 395–412. https://doi.org/10.1016/j.optmat.2003.12.025
16. Schmidt R.V., Kaminow I.P. Metal-diffused optical waveguides in $LiNbO_3$. *Applied Physics Letters*. 1974; 25(8): 458–460. https://doi.org/10.1063/1.1655547
17. Baumann I., Brinkmann R., Dinand M., Sohler W., Beckers L., Buchal C., Fleuster M., Holzbrecher H., Paulus H., Müller K.-H., Gog T., Materlik G., Witte O., Stolz H., von der Osten W. Erbium incorporation in $LiNbO_3$ by diffusion-doping. *Applied Physics A*. 1996; 64: 33–44. https://doi.org/10.1007/s003390050441
18. Jiménez-Melendo M., Haneda H., Nozawa H. Ytterbium cation diffusion in yttrium aluminum garnet (YAG) – Implications for creep mechanisms. *Journal of American Ceramic Society*. 2001; 84(10): 2356–2360. https://doi.org/10.1111/j.1151-2916.2001.tb01014.x
19. Hettrick S.J., Wilkinson J.S., Shepherd D.P. Neodymium and gadolinium diffusion in yttrium vanadate. *Journal of the Optical Society of America B*. 2002; 19(1): 123–124. https://doi.org/10.1364/JOSAB.19.000033
20. Pavlov P.V., Khokhlov A.F. Solid state physics. Moscow: Vysshaya shkola; 2000. 493 p. (In Russ.)
21. Gopal R., Calvo C. The structure of $Ca_3(VO_4)_2$. *Zeitschrift für Kristallographie – Crystalline Materials*. 1973; 137(1): 67–85. https://doi.org/10.1524/zkri.1973.137.1.67
22. Lazoryak B.I. Design of inorganic compounds with tetrahedral anions. *Russian Chemical Review*. 1996; 65(4): 287–305. https://doi.org/10.1070/RC1996v065n04ABEH000211
23. Leonidov I.A., Leonidova O.N., Surat L.L., Samigullina R. $Ca_3(VO_4)_2$–$LaVO_4$ cation conductors. *Inorganic Materials*. 2003; 39(6): 616–620. https://doi.org/10.1023/A:1024057405145
24. Rahimi Mosafer H., Paszkowicz W., Minikayev R., Kozłowski M., Diduszko R., Berkowski M. The crystal structure and thermal expansion of novel substitutionally disordered $Ca_{10}TM_{0.5}(VO_4)_7$ (TM = Co, Cu) orthovanadates. *Dalton Transactions*. 2021; 50(41): 14762–14773. https://doi.org/10.1039/D1DT02446A
25. Galakhov F.Ya. (ed.). State diagrams of refractory oxide systems. Vol. 5. Dual systems. In 4 parts. Leningrad: Nauka; 1987. Pt 3. 287 p. (In Russ.)
26. Tolkacheva A.S., Shkerin S.N., Nikonov A.V., Pershina S.V., Khavlyuk P.D., Leonidov I.I. Electrical and thermal properties of $Ca_5Mg_{4-x}Co_x(VO_4)_6$ ($0 \le x \le 4$), a promising electrode material. *Materials Letters*. 2021; 305: 130811. https://doi.org/10.1016/j.matlet.2021.130811
27. Voronina I.S., Dunaeva E.E., Papashvili A.G., Iskhakova L.D., Doroshenko M.E., Ivleva L.I. High-temperature diffusion doping as a method of fabrication of $Ca_3(VO_4)_2$:Mn single crystals. *Journal of Crystal Growth*. 2021; 563(3): 126104. https://doi.org/10.1016/j.jcrysgro.2021.126104
28. Solov'ev S.D., Korablev G.A., Kodolov V.I. Calculation of activation energy for volumetric diffusion and self-diffusion of elements in solids. Chemical Physics and Mesoscopy. 2005;7(1):31–40. (In Russ.)
29. Shannon R.D. Revised effective ionic radii and systematic studies of unteratomic distances in halides and chalcogenides. *Acta Crystallographica. Section A, Foundations of Crystallography*. 1976; 32(SEP1): 751–767. https://doi.org/10.1107/S0567739476001551